Nuclear Instruments and Methods in Physics Research A 377 (1996) 258–264

NUCLEAR INSTRUMENTS & METHODS IN PHYSICS RESEARCH Section A

ELSEVIER

Neutron induced defects in silicon detectors characterized by DLTS and TSC methods ☆

E. Fretwurst*, C. Dehn, H. Feick, P. Heydarpoor, G. Lindström, M. Moll, C. Schütze, T. Schulz

I. Institut für Experimentalphysik, Universität Hamburg, Hamburg, Germany

Abstract

Neutron induced defects in silicon detectors fabricated from n-type float zone material of different resistivity (100–6000 Ω cm) have been studied using the C-DLTS (Capacitance-Deep Level Transient Spectroscopy) and TSC (Thermally Stimulated Current) method. While the application of the C-DLTS technique for high resistivity material is limited to neutron fluences below about 10^{11} cm^{-2} the TSC method remains a powerful tool for the defect characterization even at high fluences. Up to 5 defect levels were observed in some of the unirradiated samples. These partly are due to thermal treatments during the fabrication process. After neutron irradiation defect levels at $E_c - 0.17$, -0.23 and -0.42 eV and at $E_v + 0.36$ eV were found. A detailed analysis of the predominant peak at about -0.42 eV has shown that it is a superposition of two levels at -0.39 and -0.42 eV. For these defect levels introduction rates, annealing effects and a comparison between the DLTS and TSC technique are presented. Possible correlations of these results with macroscopic detector properties are discussed.

1. Introduction

Radiation hardness studies of silicon detectors with respect to neutron induced bulk damage were mainly concentrated on investigations of macroscopic effects like the increase of the reverse current, the change of the effective impurity concentration and the degradation of the charge collection efficiency [1–3]. Much less systematic studies have been undertaken so far on the underlying microscopic effects, i.e. the induced defect levels and their correlation with the observed change of the macroscopic detector performance.

The characterization of radiation induced defects is commonly performed using the deep level transient spectroscopy (DLTS) and the thermally stimulated current technique (TSC). Both methods are sensitive to the emission process of trapped charge carriers as function of temperature which is associated with the activation energy ΔE_t, concentration N_t, and capture cross section σ_t of the involved defects.

The capacitance deep level transient spectroscopy (C-DLTS) is a very sensitive method for the detection and characterisation of deep defect levels. But it is well known that the application of this technique for high resistivity detector grade n-type silicon is limited by the requirement $N_t/N_s \ll 1$, where N_t is the concentration of deep levels and N_s the net doping concentration [4]. This requirement implicates an upper limit for the neutron fluence which a device can be exposed to without serious distortions of the capacitance transients (see e.g. Ref. [5]). Another powerful tool is the TSC-technique which is not limited by such a restriction and can be used for the defect characterization after irradiations with high fluences (see e.g. Ref. [6]).

In this paper results obtained by the C-DLTS and TSC method for neutron induced defects are compared with each other. The individual introduction rates have been measured and first annealing studies are reported and discussed.

2. Experimental procedure

The investigated diodes were fabricated from n-type float zone material (Wacker Chemitronic) of different resistivity in the range between 100 Ω cm and 8 kΩ cm using both the surface barrier and the ion implantation technique. Table 1 summarizes the main parameters of the material, type of diodes and thermal treatment during fabrication.

The irradiations were performed at the following facilities: (a) At the Physikalisch-Technische-Bundesantalt Braunschweig (PTB) using the d + Be reaction for the production of a high intensity neutron beam with a mean energy of 5.3 MeV [9]. (b) At the University Hospital

☆ Work supported by the BMFT under contract 05 6 HH 17P.

* Corresponding author. Tel. +49 40 4123 4426, fax +49 40 4123 6571.

SSDI 0168-9002(95)01405-5

Table 1
Used silicon material, type of diodes and thermal treatment during fabrication

	Wafer number			
	941	M2	93A	938
Doping concentration [cm^{-3}]	7.0×10^{11}	2.0×10^{12}	3.1×10^{12}	4.1×10^{13}
Type of diode	surface barrier[a]	ion implanted[b]	surface barrier[a]	surface barrier[a]
Diode area [cm^2]	0.44/0.16	0.25	0.44	0.44
Oxide passivated (therm. treatm.)	yes	yes	no	no
Guard ring	no	yes[c]	no	no

[a] Detectors fabricated at Hamburg University [7].
[b] Detectors fabricated by the MPI-Halbleiterlabor, München [8].
[c] Always floating throughout the experiments.

Hamburg (UKE) using the T(d, n) reaction which delivers 14.1 MeV monoenergetic neutrons [10]. The particle fluences given in this report are normalized to equivalent 1 MeV neutron values (for details see Ref. [11]).

A commercially available DLTFS-apparatus [12] was used for the defect characterization in the low fluence range (below $10^{12}\,cm^{-2}$). The computer controlled setup allows the recording of the entire capacitance transients and a subsequent analysis by a fast-Fourier-transform algorithm which results in up to 16 coefficients. Thus, a sufficient reduction of the primary data is achieved and a fast recognition of non-exponential transients which may e.g. be caused by closely neighbouring levels is possible allowing a real time rejection of the transient data for those cases. In contrast to the original Lang method the most striking advantage of this new technique lies in the fact that only a single temperature scan is needed for a sufficient defect characterization i.e. ΔE_t, N_t, and σ_t. In addition several time-bases and pulsing-schemes are available. We have been typically working with 1 ms pulses and time-bases of 20 ms, 200 ms, and 2 s. For the DLTS experiments both a liquid N_2 and a He cryostat were available. A more detailed description of the system can be found elsewhere [13].

The TSC-technique makes use of the thermally stimulated emission current of trapped charge carriers in the space charge region of the detector. As long as the traps can be filled by available charge carriers at low temperature (20 K) and a revere bias above total depletion can be applied, the TSC-technique can be used for the defect characterization including the evaluation of the trap concentration of even highly damaged detectors. One shortcoming of this method is that numerous temperature scans have to be performed in order to extract sufficient data for the activation energy and the capture cross section of the observed defect levels. This can be obtained by delayed heating measurements or recording of TSC-scans with different temperature rates $\beta = dT/dt$ [14,15]. A special problem of highly damaged detectors is the filling process at low temperatures. In our experiments sufficiently high injection of charge carriers could only be achieved for ion implanted detectors by forward biasing up to several volts. Typically a current of 2.5 mA was injected for 20 s ensuring a complete filling of all traps. For TSC-measurements the used He-cryostat allows heating rates up to about $\beta = 0.8$ K/s in the temperature range between 20 and 200 K.

3. Experimental results and discussion

3.1. DLTS-studies

For an easy assignment the different observed peaks are labeled by the letter E or H with consecutive numbers for electron respectively hole traps. Up to 5 defect levels were detected in unirradiated samples (see Table 2). Fig. 1 demonstrates as an example 2 DLTS-spectra for samples differing in the doping concentration and thermal treatment during the fabrication process. Similar defect levels – especially E5 and E7 – were reported by Verbitskaja et al. [16] investigating the influence of different heat treatments on the formation of defects. While the level E5 seems to be correlated with the oxidation process, the level E7 is also observed for a sample processed without any oxidation. So far an assignment to known defects is not possible. It

Table 2
Defect levels measured before irradiation. In the samples from the wafers #M2 and #938 (see Table 1) no preirradiated levels were detected

			Trap concentration N_t [$10^{10}\,cm^{-3}$]	
Defect	ΔE_t [ev]	σ_t [cm^2]	#941	#93A
E1	−0.06	6×10^{-16}	≈0.3	–
E2	−0.12	1×10^{-14}	≈0.3	0.40±0.06
E4	−0.23	1×10^{-14}	0.54±0.15	–
E5	−0.26	1×10^{-17}	2.20±1.04	–
E7	−0.53	3×10^{-15}	2.92±1.23	1.59±0.32

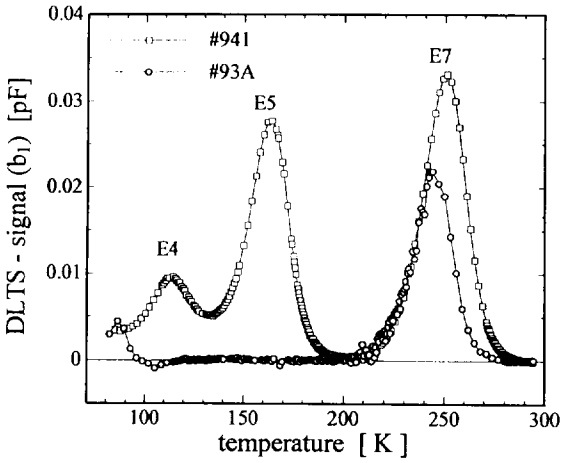

Fig. 1. DLTS spectra (first sin-coefficient b_1) for two unirradiated samples. The sample #941 was oxide passivated while the sample #93A was not.

should however be noted that these defects showing up in the preirradiated detectors are not always present. The detectors from the low resistivity wafer #938 and those processed at the MPI-Munich (wafer #M2, see Table 1) do not show such an effect at all.

After neutron irradiation mainly 3 electron traps at about

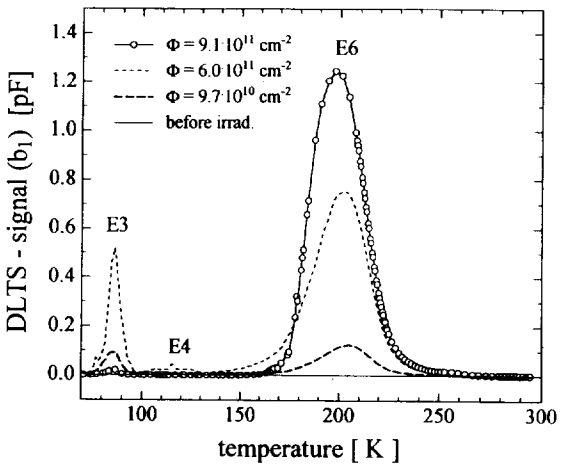

Fig. 2. DLTS spectra of three samples (wafer #M2) before and after irradiation with different fluences.

−0.17 eV (E3), −0.23 eV (E4) and −0.42 eV (E6) were found. Fig. 2 presents spectra obtained before and after irradiation for ion implanted diodes. The spectrum measured after exposure to the highest fluence of 9×10^{11} cm^{-2} shows a strongly reduced E3 amplitude and a distorted peak shape for E6. This is an indication that in this case the DLTS-requirement $N_T/N_s \ll 1$ is not fulfilled anymore. The dependence of the E6 resp. E3 concentration on the neutron fluence is shown in Figs. 3a and 3b for samples from the different wafers under investigation (see Table 1). The resulting introduction rates and defect parameters are summarized in Table 3. The hole trap H1 can only be measured with ion implanted devices because an injection of holes is not possible in Schottky diodes. A variation of filling lengths has shown that it is not always possible to completely fill the level E4 within 1 ms. Since all data presented in this paper were obtained with a 1 ms filling pulse the E4 introduction rates are not given.

Although in the case of the Schottky diodes the effective impurity concentration before irradiation is ranging over about 2 orders of magnitude the resulting introduction rates for E3 and E6 show only little deviations (Table 3 and Fig. 3). In contrast to this, the measurements with the ion implanted diodes lead to values which are 1.5 to 2 times higher. It should be noted that these diodes have a guard ring which was however floating during the experiments. It is well known, that for such a structure the lateral field extends beyond the central diode electrode above "punch through" occurring close to 50 V [17]. Unfortunately the DLTS-apparatus is limited to voltages below 20 V. Therefore, measurements above the "punch through" were not possible and the determined defect concentration is expected to be affected by a high uncertainty.

A more detailed analysis of the E6 and the corresponding transients show that this peak is not caused by a single level. Its shape can only be reproduced by a superposition of 2 levels. Fitting simulated spectra to the measured data of all Fourier-coefficients by the eye (up to 16 spectra for one temperature scan) the parameters of both levels were optimized (see Table 4). This method turns out to be quite reliable since comparable results were obtained for different measurements. The accuracy of the level energy and the capture cross section is estimated to be 0.5% and 30%, respectively [18]. Fig. 4 presents the result for such a fit for one of the Fourier-coefficients in

Table 3
Neutron induced electron and hole traps and corresponding introduction rates observed by the DLTS-technique for fluences below $\phi = 1\times 10^{12}$ cm^{-2}. The hole trap H1 could only be measured in the wafer #M2 (see text).

Defect	ΔE_t [eV]	σ_t [cm^2]	Introduction rate [cm^{-1}]			
			#941	#M2	#93A	#938
E3	−0.17	1×10^{-14}	0.56±0.06	1.00±0.06	0.45±0.15	0.51±0.05
E6	−0.42	2×10^{-15}	0.66±0.09	0.87±0.01	0.62±0.10	0.64±0.08
H1	+0.36	2×10^{-15}	–	1.19±0.09	–	–

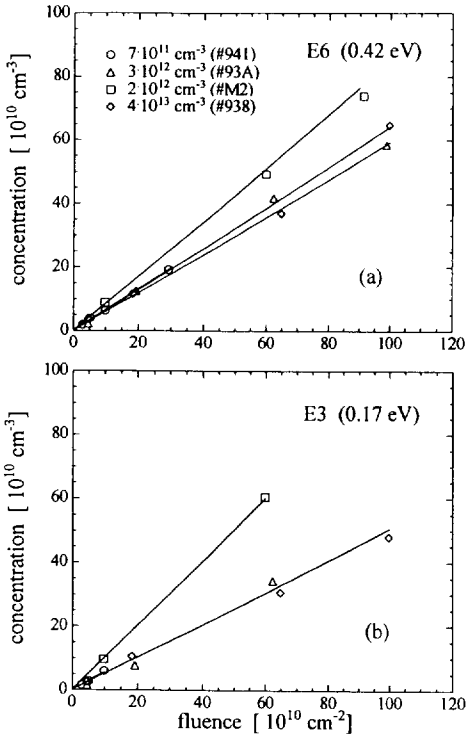

Fig. 3. Defect concentration versus fluence for (a) the E6 and (b) the E3 level. The different symbols indicate the initial effective doping concentration (see also Table 2).

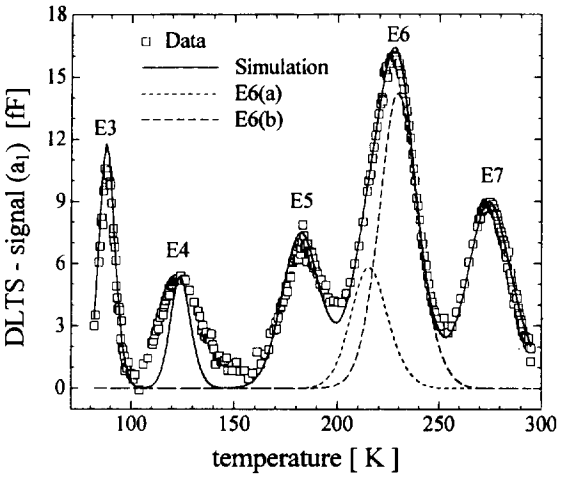

Fig. 4. Comparison between simulated DLTS spectrum and experimental data (first cos-coefficient a_1). The peak E6 can be reproduced only by the superposition of two levels (see text).

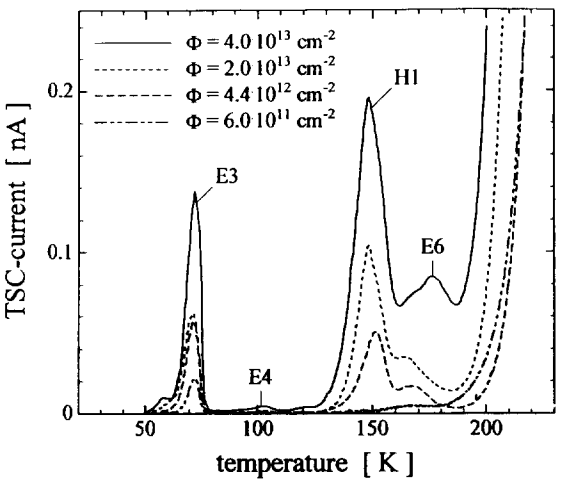

Fig. 5. TSC spectra for numerous fluences (wafer #M2).

comparison to the experimental data including the strong background peaks E5 and E7 (see above).

3.2. TSC-measurements

Spectra obtained by TSC-measurements for ion implanted detectors (wafer #M2) exposed to fluences in a wide range up to $4 \times 10^{13}\,\mathrm{cm}^{-2}$ are demonstrated in Fig. 5. The pronounced peak occurring at a temperature of about 70 K is associated with the E3 level found in the DLTS spectra. The dominant peak at about 150 K is assumed to be a hole trap and, therefore, assigned by H1 and the adjacent broad peak centered at about 170 K fits with the DLTS-peak E6. These assignments were derived from a comparison of TSC- and DLTS-spectra measured for one sample which was exposed to a low fluence of $\phi = 1 \times 10^{11}\,\mathrm{cm}^{-2}$ (see Fig. 6). While for the DLTS-spectrum electron and hole traps could be measured separately by means of the sign of the transient (compare Fig. 6 upper part) the TSC measurement does not furnish a corresponding information (see Fig. 6 lower part). Making use of the level parameters (activation energy and cross section) extracted from the DLTS-measurement the TSC-signal could be simulated by merely adjusting the trap

Table 4
Activation energies, cross sections and introduction rates for the defect levels E6-a and E6-b. The DLTS measurements were performed for fluences lower than $\phi = 1 \times 10^{12}\,\mathrm{cm}^{-2}$

			Introduction rate [cm^{-1}]			
Defect	ΔE_t [eV]	σ_t [cm^2]	#941	#M2	#93A	#938
E6-a	−0.39	1×10^{-15}	0.30±0.06	0.40±0.02	0.20±0.04	0.23±0.03
E6-b	−0.42	1×10^{-15}	0.59±0.05	0.75±0.11	0.45±0.02	0.54±0.05

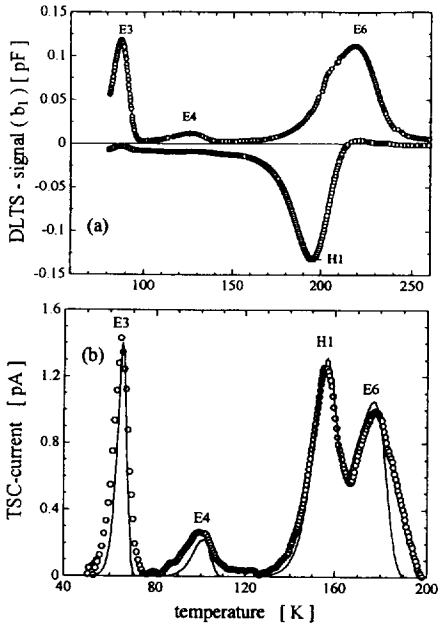

Fig. 6. (a) DLTS spectra after electron (upper part) and hole injection (lower part). (b) Comparison between a measured and a simulated TSC spectrum. The parameters for the simulation were extracted from the DLTS-measurement.

concentrations (solid line in Fig. 6). The trap concentrations as determined by the DLTS measurement have not been used due to the problems arising from the guard ring of this sample.

The trap concentrations can be derived from the TSC measurements with high accuracy by simply integrating over the corresponding peak and normalizing to the detector volume assuming the device is fully depleted. The extracted concentrations for the E3 and H1 peak as function of fluence are plotted in Fig. 7. At low fluences (below 10^{12} n/cm^2) the increase of the E3 concentration is proportional to ϕ as obtained by the DLTS-measurements (compare Fig. 3b). However the introduction rate for E3 is found to be 0.44 cm^{-1} instead of 1.0 cm^{-1} for the DLTS measurement. The same factor of 0.5 appears for the introduction rate of H1 measured by TSC (0.60 cm^{-1}) and DLTS (1.2 cm^{-1}, see Table 3). In contrast to this, the results obtained by both methods coincide very well for the Schottky diodes (see Table 3). This is an additional indication that the DLTS measurements for the samples of the wafer #M2 suffer from the uncertainty in the determination of the effective doping concentration (see preceding paragraph).

At high fluences (above 3×10^{12} n/cm^2) much lower slopes of the trap concentrations as function of ϕ are observed (see Fig. 7). The according values for the E3 and H1 peaks are 0.03 cm^{-1} and 0.20 cm^{-1}, respectively. Although the measured data are in quite good agreement with the results reported by Biggeri et al. [19] there is still

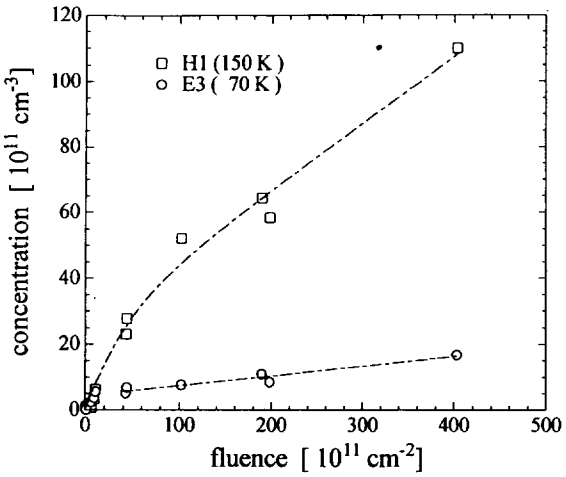

Fig. 7. Concentration of the TSC peaks H1 and E3 versus fluence (see also Fig. 5).

some uncertainty in the reliability of the absolute defect concentration for high fluences. It was observed that the extracted trap concentrations depend on the used reverse bias voltage which was chosen to be just above the depletion voltage, which however was derived from room temperature *CV* measurements. An altered full depletion voltage at low temperatures may come about because of a freezing of trapped charges at lower temperatures [20].

3.3. Annealing studies

The DLTS spectrum of an ion implanted detector (wafer #M2, see Table 1) which was irradiated with neutrons (6.0×10^{11} n/cm^2) has been monitored in an isochronal annealing study (Fig. 8). The temperature was raised from 353 to 493 K in 20 K steps each annealing lasting 20

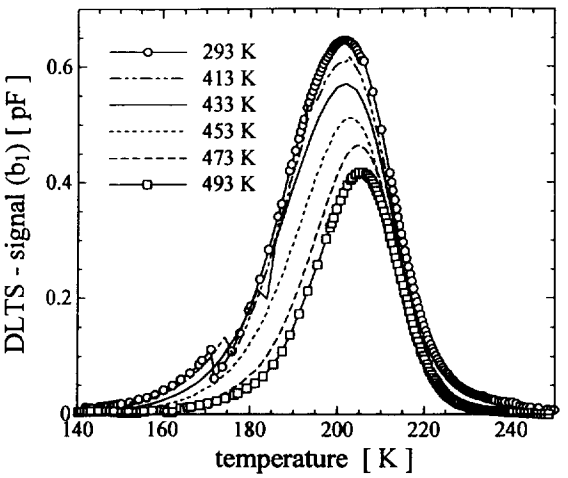

Fig. 8. Decrease of the E6 peak in an isochronal heat treatment (sample #M2, $\phi_{eq} = 6 \times 10^{11}$ cm^{-2}).

minutes. A reduction of the E6 peak amplitude is obvious but also a shift of the peak position towards higher temperatures is seen. The shift may be attributed to a different annealing behavior of the two constituents which were already separated using the fitting method discussed in Section 3.1. Indeed the E6 peak measured after the 493 K annealing step can be described by a single level with an energy of −0.42 eV as already was found for E6-b in Table 4. This implies that the second component has almost annealed out. Hence, the corresponding level may be investigated by applying the DLTS-analysis to the subtraction of the post anneal spectra from the initial spectrum. It is reassuring that this procedure leads to an assignment of −0.39 eV, also identical with the energy of the E6-a level given in Table 4. The annealing behaviour of the dominant centers E3, E6 and H1 is summarized in Fig. 9. While the peak analysis of E6 leads to a decrease of its concentration by about 35% with respect to the value before tempering, the E3 peak shows a slight increase of 13% in the temperature range between 293 and 493 K. For the hole trap only small variations of the concentration are observed.

3.4. Conclusions

It is generally assumed that the formation of stable defects in neutron irradiated silicon is dominated by vacancy related centers like VO, VP, V_2 and higher order vacancy complexes and by Si interstitials. Because the carbon concentration in high resistivity material is in the order of $10^{15}\,cm^{-3}$ we expect the release of C_i as a consequence of the irradiation by the reaction $Si_i + C_S \rightarrow Si_S + C_i$ as outlined in Ref. [21]. C_i is known to be mobile in the lattice at room temperature and therefore secondary reactions are possible [22–25]:

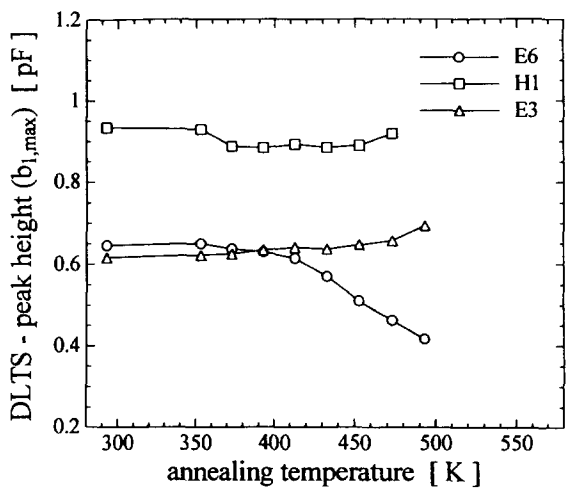

Fig. 9. Isochronal annealing behaviour of the E3, E6 and H1 peaks. For peak E6 see also Fig. 8.

Table 5
DLTS- and TSC-peaks observed in this work and conceivable assignments with defects [23,25,26]

Defect	ΔE_t [eV]	Identification
E3	−0.17	A-center (VO) + C_iC_s
E4	−0.23	V_2^- + unknown
E6	−0.42	V_2^- + E-center (VP) + unknown
H1	+0.36	C_iO_i

$C_i + C_S \rightarrow C_iC_S$, $C_i + O_i \rightarrow C_iO_i$ or $C_i + P_S \rightarrow C_iP_S$.

Finally Table 5 summarizes the corresponding assignments conceivable with the DLTS- and TSC-peaks measured here. Similar defect levels in neutron irradiated high resistivity silicon were reported by different groups [6,27–29]. Much less is known about the levels that are present before irradiation. More information would be desireable since a significant background signal is introduced complicating a systematic study (see Fig. 4).

We have shown that the DLTS and TSC methods give similar results in the low ϕ region. Therefore, the failure of the defect characterization by C-DLTS measurements due to the $N_T \ll N_S$ restriction may be overcome by extending the defect analysis towards higher fluences using the TSC method. The corresponding introduction rates, however, exhibit an unexpected behavior and more measurements are needed for clarification.

Referring to the arguments that so far had been used in the literature to explain the macroscopic change of the effective doping concentration in terms of a donor removal and the reverse annealing in terms of an appearing acceptor we want to stress the following two points.

If phosphor removal according to a model $N_D(\phi) = N_{D0}\exp(-c\phi)$ (compare Ref. [30]) would occur with a removal rate c close to $10^{-13}\,cm^2$ and the initial phosphor concentration N_{D0} then the E-center introduction rate g_E for low fluence irradiations could be written $N_{D0}c$. Thus, for high resistivity material ($N_{D0} = 10^{12}\,cm^{-3}$) we would expect $g_E \approx 0.1\,cm^{-1}$ and for the investigated low resistivity material ($N_{D0} = 4 \times 10^{13}\,cm^{-3}$) $g_E \approx 4\,cm^{-1}$, provided the approach may be extrapolated to lower resistivity material. The introduction rate found for the level E6, however, was found to be independent of the initial doping concentration and is of the order of $0.6\,cm^{-1}$. Therefore, the macroscopic result most likely is not due to the mere creation of V–P centers but other competing processes may play a role. Moreover, it was observed in this study that the E6 component E6-b which energetically could be assigned to the VP-complex (E-center) does not show any annealing effect at high temperatures, although the annealing temperature of the E-center is known to be around 400 K for 10 Ω cm resistivity material and tends to decrease for higher resistivity samples [31]. Thus we suggest that the E6-b level represents the singly charged divacancy VV^- for which the annealing temperature of 570 K was not reached in our experiment [32].

The reverse annealing effect, on the other hand, would require the formation of an acceptor like defect that is negatively charged in the depletion region. Thus, this level must be located in the lower half of the band gap [4] and should give rise to a DLTS signal corresponding to a hole trap. During the annealing experiment, however, the concentration of the only hole trap H1 observed does not show a significant increase. But the reverse annealing also could be due to an acceptor level that has not been detected in our measurements because it is too shallow. Furthermore, the macroscopic antiannealing effect, i.e. the space charge becoming more negative, could be explained by a donor in the upper half of the band gap that anneals out. This actually is seen for the E6-a peak, but the generation rate of around $0.2\,cm^{-1}$ is larger by a factor of 4 compared to the macroscopic value of about $0.05\,cm^{-1}$ [11]. Anyhow, the general behavior of radiation induced defects is to produce acceptor levels in the upper half and donor levels in the lower half of the band gap. This for instance is believed for the C_iO_i level that we have associated with the H1 peak at $E_v + 0.36$ eV (Table 5) [24] and also may be assumed for the E6-a level. Thus, we suggest that neither the H1 nor the E6-a level contributes to the reverse annealing of the effective doping concentration observed in macroscopic measurements.

References

[1] The RD2 Collaboration, RD-2 Status Report, CERN/DRDC 94-34.

[2] The RD20 Collaboration, RD20/STATUS REPORT, CERN/DRDC94-39.

[3] Z. Li, Nucl. Instr. and Meth. A 360 (1995) 445 and literature cited here.

[4] D.V. Lang, J. Appl. Phys. 45 (1974) 3023.

[5] V. Eremin et al., Detection mechanism of radiation induced defect levels in high resistivity silicon by DLTS method with preliminary filling pulse, to be published in J. Appl. Phys.

[6] M. Bruzzi et al., Nucl. Instr. and Meth. A 352 (1995) 618.

[7] E. Fretwurst et al., Nucl. Instr. and Meth. A 288 (1990) 1.

[8] G. Lutz, MPI-Halbleiterlabor, München and J. Kemmer, Ketek Gmbh, München, private communication.

[9] H.J. Brede et al., Nucl. Instr. and Meth. A 274 (1989) 332.

[10] R. Schmidt et al., Med. Phys. 7 (1980) 507.

[11] H. Feick et al., these Proceedings. (7th Europ. Symp. on Semiconductor Detectors, Schloss Elmau, Bavaria, Germany, 1995) Nucl. Instr. and Meth. A. 377 (1996) 217.

[12] Dr. L. Cohausz, Halbleitermeßtechnik Gmbh, Moosburg.

[13] S. Weiss, Ph.D. thesis, University Kassel (1991).

[14] J.C. Muller et al., Solid-State Electronics 17 (1974) 1293.

[15] M.G. Buehler, Solid-State Electronics 15 (1972) 69.

[16] E.M. Verbitskaya et al., Sov. Phys. Semicond. 26(11) (1992) 1101.

[17] R. Wunstorf et al., Ref. [11], p. 290.

[18] C. Dehn, Diploma thesis, Universität Hamburg (1995).

[19] U. Biggeri et al., IEEE Trans. Nucl. Sci. NS-41(4) (1994) 964.

[20] V. Eremin et al., Nucl. Instr. and Meth. A 360 (1995) 458.

[21] M.T. Asom et al., Appl. Phys. Lett. 51(4) (1987) 256.

[22] X.D. Zhan and G.D. Watkins, Phys. Rev. B47(11) (1993) 6363.

[23] L.W. Song et al., Phys. Rev. B42(9) (1990) 5765.

[24] L.W. Song and G.D. Watkins, Phys. Rev. B42(9) (1990) 5759.

[25] J.M. Trombetta and G.D. Watkins, Appl. Phys. Lett. 51(14) (1987) 1103.

[26] Landolt-Börnstein, Impurities and Defects in Group IV Elements and III-V Compounds, Vol. 22b (Springer, 1989).

[27] J. Matheson et al., RD20 Technical Report TN/36 1995.

[28] V. Eremin et al., IEEE Trans. Nucl. Sci. NS-42(4) (1995) 387.

[29] M. Bosetti et al., Nucl. Instr. and Meth. A 361 (1995) 461.

[30] R. Wunstorf, Ph.D. thesis, Universität Hamburg, see also DESY FH1K-92-01 (1992).

[31] L.C. Kimerling et al., Phys. Rev. B3(2) (1971) 427.

[32] G.D. Watkins and J.W. Corbett, Phys. Rev. 138(2) (1965) A543.